

Published in final edited form as:

Mol Cancer Ther. 2014 December ; 13(12): 2805–2816. doi:10.1158/1535-7163.MCT-13-1091.

Inhibition of Monocarboxylate transporter-1 (MCT1) by AZD3965 enhances radiosensitivity by reducing lactate transport

Becky M. Bola^{1,2}, Amy L. Chadwick^{1,3}, Filippos Michopoulos⁴, Kathryn G. Blount¹, Brian A. Telfer¹, Kaye J. Williams¹, Paul D Smith⁴, Susan E. Critchlow⁴, and Ian J. Stratford^{1,*}

¹Manchester Pharmacy School, Manchester Cancer Research Centre, University of Manchester, Manchester M13 9PT, UK

²Clinical and Experimental Pharmacology, CR-UK Manchester Institute, Manchester, M20 4BX UK

³Breakthrough Breast Cancer, Institute of Cancer Sciences, University of Manchester, Manchester M20 4BX, UK

⁴Oncology iMED, AstraZeneca, Mereside, Alderley Park, Macclesfield, Cheshire, SK10 4TG, UK

Abstract

Inhibition of the monocarboxylate transporter MCT1 by AZD3965 results in an increase in glycolysis in human tumour cell lines and xenografts. This is indicated by changes in the levels of specific glycolytic metabolites and in changes in glycolytic enzyme kinetics. These drug-induced metabolic changes translate into an inhibition of tumour growth *in vivo*. Thus, we combined AZD3965 with fractionated radiation to treat SCLC xenografts and showed that the combination provided a significantly greater therapeutic effect than the use of either modality alone. These results strongly support the notion of combining MCT1 inhibition with radiotherapy in the treatment of SCLC and other solid tumours.

Keywords

Metabolism; AZD3965; MCT1; Lactate; Radiotherapy

Introduction

The presence of hypoxia is a microenvironmental characteristic of the majority of solid tumours. A hypoxic microenvironment is associated with malignant progression, development of metastases and presents a challenge for conventional cancer therapeutics [1-4]. In addition to genetic changes acquired during tumour development, micro-environmental constraints can dictate the adaptive metabolic pathways used within a

*Corresponding Author: Professor Ian J Stratford, Manchester Pharmacy School, University of Manchester, Room 2.018, Stopford Building, Oxford Road, Manchester, M13 9PT, UK. Tel: +44(0)161-275-2387 Fax: +44(0)161-275-2416 ian.stratford@manchester.ac.uk.

Conflict of interest notification: FM, PDS and SEC are full time employees and stockholders of AstraZeneca plc. IJS is in receipt of research support from AstraZeneca.

tumour. In particular, tumour hypoxia can direct the metabolic phenotype towards glycolysis. This glycolytic adaptation can persist even in the presence of oxygen where it is referred to as the Warburg effect [5]. This altered metabolic phenotype has recently been identified as an emerging hallmark of cancer [6]. Increased glycolysis results in the generation of lactate, this is not only a waste product of increased glycolytic rate, but it is also thought to act as a signalling molecule, an antioxidant, and is reported to enhance immune escape [7]. Consequently, increased tumour hypoxia, glycolytic rate and lactate concentration are linked with tumour aggressiveness, treatment failure and metastasis. In fact, lactate itself is a powerful independent prognostic indicator of disease progression, metastasis and reduced survival in many tumour types [8-12].

Lactate production results in a requirement for lactate transport, both to prevent lactate accumulation and to provide a respiratory substrate. The majority of lactate transport occurs via the family of proton linked monocarboxylate transporters (MCTs) that are responsible for the facilitated diffusion of a carboxylate ion and a proton across the plasma membrane. This transport is not an active process and is reliant on the overall concentration gradient of the metabolite [13, 14]. Of this family, MCT1 and MCT4 are the predominantly expressed isoforms in cancer. MCT1 has a ubiquitous expression pattern and mediates the bidirectional high affinity transport of monocarboxylates including L-lactate, pyruvate, acetate and D,L- β -hydroxybutyrate [15]. In contrast, MCT4 is hypoxia regulated; it has a lower affinity for lactate, a higher turnover rate and is adapted towards lactate efflux in glycolytic cells [16, 17].

Lactate lost from one cell population can be taken up and used as a respiratory substrate in others. This metabolic co-operation is seen in some normal tissues such as in fast twitch muscle fibres ([18-20] and between neurons and glia [21-23]. Analogous to this, increasing evidence suggests that lactate shuttling may play an important role in tumour growth and metastasis. Sonveaux *et al.* [24] hypothesised that a metabolic symbiosis may exist in solid tumours whereby lactate produced during glycolysis in the hypoxic tumour cell compartment is preferentially taken up by the oxygenated tumour cell population and used as a fuel source for oxidative metabolism. Similarly, it has been suggested that metabolic coupling may occur between aerobic tumour cells and the cancer-associated stroma within multiple cancer types including cancers of the breast [5] ovary [25] and prostate [26]. In this model, tumour cells are able to induce oxidative stress, glycolysis, up-regulation of MCT4 and lactate efflux in cancer-associated fibroblasts, providing metabolic substrates for aerobic MCT1-expressing epithelial tumour cells. The transport of lactate is therefore critical to the maintenance of the symbiotic micro-environment and MCT1 is identified as the major transporter involved in lactate influx into tumour cells. In addition to the important functional role of MCT1 in tumour metabolism, MCT1 protein expression in tumours has been linked with variables associated with disease progression and prognosis in a variety of tumour types including breast [27] ovarian [28], gastric [29] and colorectal cancer [30].

For these reasons, MCT1 is an attractive therapeutic target for inhibiting the metabolic interplay between cell populations within tumours. The non-specific MCT1 inhibitor α -cyano-4-hydroxycinnamate (CHC) has been reported to produce anti-tumour effects by interfering with this metabolic coupling, by inhibiting lactate uptake into oxygenated tumour

cells, increasing glucose uptake, and indirectly starving hypoxic tumour cells of glucose [24]. In addition, CHC has been shown to increase necrosis and alter tumour volume *in vivo* [31-33]. However, CHC is not a specific MCT1 inhibitor and as a consequence these data should be interpreted with caution [34, 35].

Specific inhibitors with greater inhibitory potency and selectivity towards MCT1 have been developed for use in immunosuppression [36, 37], and these have been shown to influence lactate transport [38]. Recent improvements on these compounds have resulted in the generation, by AstraZeneca, of AZD3965. This compound is a selective MCT1 inhibitor; it inhibits MCT1 with a binding affinity 1.6 nM and it is 6 fold selective over MCT2 and does not inhibit MCT3 or 4 at 10 μ M concentrations [39]. In addition, the compound has good oral bioavailability, and it has entered phase I clinical trial for treatment of advanced solid tumours [40].

In this study, we evaluate the metabolic and therapeutic effects of AZD3965 in small cell lung cancer and gastric cancer cell lines. In particular, we demonstrate the ability of AZD3965 to inhibit both lactate efflux and influx into cells and cause an increase in glycolysis and an up-regulation of glycolytic enzymes. These changes were sufficient to inhibit tumour growth *in vivo*. In addition, we combined AZD3965 with radiotherapy *in vivo* and showed that the combined treatment produced a substantially greater anti-tumour effect than either modality when used alone.

Materials and Methods

Cells

DMS114, and H526 small cell lung cancer cells and HGC27 gastric cancer cells were maintained in RPMI1640 with 10% FCS and 1% L-glutamine (complete media). Cell lines were chosen on the basis of relatively high sensitivity to AZD3965 [39]. DMS114 and HGC27 cells were obtained from AstraZeneca and H526 cells were provided by the CR-UK Manchester Institute. All cells were subsequently authenticated while used in the University of Manchester laboratories by the use of an in-house DNA sequencing and authentication service. Cells were also shown to be mycoplasma free during the course of this work. For all experiments, cells were plated overnight prior to treatment with AZD3965 and/or different oxygen concentrations for a further 24hr (unless an alternative treatment time is indicated). Some experiments also included exposure to cobalt chloride as a hypoxia-mimetic. Cobalt chloride is able to mimic hypoxia by preventing HIF degradation, this is at least partially due to its occupation of the VHL-binding domain of HIF-1 α thus preventing its degradation [41].

Glucose and Lactate uptake assay

After treatment cells were washed prior to the addition of uptake cocktail consisting of buffer (25mM glucose, 137mM NaCl, 5.37mM KCl, 0.3mM Na₂HPO₄, 0.44mM KH₂PO₄, 4.17mM NaHCO₃, 1.26mM CaCl₂, 0.8mM MgSO₄, 10mM HEPES pH 7.4) containing 100nM AZD3965 or equivalent volume of DMSO vehicle. For the glucose and lactate assays, 2mM glucose and ³H-2-deoxyglucose at an activity of 2 μ Ci and ¹⁴C-lactate at an

activity of 0.2 μ Ci were added respectively and incubated for one hour at 37°C. Subsequently, the cocktail was removed and the cells washed and lysed in 0.5ml of lysis buffer (0.1% SDS and 0.1% Triton-X in HEPES buffer); 0.4ml of this was transferred to a scintillation vial with 4ml of scintillation fluid (Ecoscint A, National Diagnostics), the addition of 0.4ml of the original lactate or glucose cocktail was used as a positive control, to establish the total amount of radioactive metabolite added. The remaining 100 μ l was used for a protein assay. The uptake was normalised to both the amount of radioactive metabolite present in the media (positive control) and also to protein concentration, to control for variation in cell number which may have been caused as a result of the treatments.

Lactate, ATP and GSH/GSSG assay

Lactate concentration was determined by colorimetric assay (Trinity Biotech, Bray, Ireland) and compared to a standard curve of known lactate concentrations. The lactate present as a result of efflux from the cell was determined by measuring cell free samples and deducting the amount of lactate originally in the media (derived from the FCS). Intracellular lactate was evaluated using the same assay; cells were washed in PBS prior to lysis in Tris/NaCl lysis buffer (20mM Tris, 150mM NaCl, 1% Triton-X100, pH 7.6).

The ATP concentration in cell lysates was determined by a luminescent assay (ENLITEN ATP system, Promega, Southampton, UK) and comparison made to the cellular ATP concentrations in lysates derived from untreated normoxic controls.

GSH and GSSG concentrations were determined in the same lysates by GSH/GSSG-Glo luminescent assay (Promega, Southampton, UK).

Assay of Reactive Oxygen Species

Following treatment cells were re-suspended in PBS and stained with 10 μ M carboxy-DCFDA (Molecular Probes, Invitrogen), washed and then 10,000 events within a population gated to only include live cells was analysed by FACs (Cyan ADP flow cytometer, Ely, UK). Mean fluorescence in the live cell population was compared against the control for each oxygen tension and drug concentration.

Metabolomics

Cells were plated and allowed to adhere before washing and exchanging the media for one containing dialysed FCS devoid of constituents smaller than 1000amu such as small sugars and lactate (Sigma Aldrich). Hypoxic (1% oxygen) experiments were conducted in a hypoxic cabinet (Ruskinn Sci-tive-N). Samples were treated with DMSO vehicle, 10nM or 1 μ M AZD3965 for 6 or 24hrs under normoxic or hypoxic conditions. To extract the metabolites media was removed and 400 μ l (-20°C) 40:40:20 acetonitrile: methanol: water added immediately to quench metabolism and extract metabolites. The plates were then kept on dry ice for 20 minutes prior to scraping the cell:solvent mixture into chilled tubes, precipitated proteins were then removed by centrifugation and the supernatant stored at -20°C. As an LC-MS quality control, a pooled sample (QC) was generated containing equal quantities of each sample. Samples (100 μ l) and the pooled sample were evaporated using a SpeedVac Savant 1010 (Thermo Scientific), with no heat, for 60 min. Subsequently,

metabolites were re-suspended in 50 μ l deionised water. For the liquid chromatography a Dionex U3000 RS pump was operated at 400 μ l/min and the column maintained at 60°C. Liquid Chromatography used: Buffer A, 10mM tributylamine, 15mM Acetic acid in water; and Buffer B, 20% isopropanol in methanol; Column: Waters Acquity HSS C18 100 \times 2.1mm, 1.7 μ m particles. Metabolites were eluted following a gradient profile starting at 0-0.5min at 0%B changing after 4min to 5%B, 6min 5%B, 6.5min 20%B, 8.5min 20%B, 14min 55%B, 15min to 100%B and column flushed with 100%B for another two minutes before changing to 100%A for 3min re-equilibration prior to next injection. After the column was conditioned using 10 injections of the pooled sample, all samples were analysed in random order on a 4000 Qtrap mass spectrometer using negative ionisation. A QC sample was injected every 10 samples to monitor instrument variability. Subsequently, peak integration was performed using the MultiQuant software and all sample peaks were compared to the standards (and standards + QC mix to ensure that the correct peak was selected). Data was further scaled to log base 2 and normalised to median sample metabolic profile. Coefficients of variation (CVs, $\text{stdev}/\text{mean} \times 100$) were calculated for each QC analyte. Fold-changes, F-test and T-Tests between groups were calculated using Excel. Metabolites are considered to have changed when they met the following criteria: a) QC CV<30; b) p-value<0.05 and absolute \log_2 (fold change)>0.5 (log fold change calculated using the following formula: $(\text{average}(\text{treated})) - (\text{average}(\text{group}(\text{DMSO control})))$).

Determination of glycolytic enzyme kinetics

Cells were plated overnight and treated with 100nM AZD3965 or vehicle for 24 hours. The cells were then washed, once in PBS and twice with lysis buffer (50mM Mops, 100mM KCl, 5mM MgCl₂, 1mM EDTA, 0.1mM DTT, 1mM PMSF supplemented with 1 \times mini complete protease inhibitor cocktail tablets (Roche). The cells were harvested by scraping and centrifugation, and the pellet snap frozen without buffer in liquid nitrogen. Frozen aliquots of cells were thawed on ice and re-suspended in lysis buffer. Cells were lysed by 3 rounds of freezing in liquid nitrogen and thawing at 37°C for 2 minutes each. Lysates were subsequently centrifuged (13,000g, 10min, 4°C) until clear and then stored on ice. Enzyme activity in the cell lysates was determined using a micro-plate reader (Anthos Zenyth 3100) to measure either production or depletion of NADH/NADPH, through its absorbance at 340/10 nm, occurring as a result of direct or coupled enzyme reactions. The 96-well plates used for the assays were pre-heated to 37°C for 10 minutes prior to starting reactions, initiated by the addition of 5 μ l cell lysate to 95 μ l of reaction buffer (50mM Mops pH 7.4, 100mM KCl, 5mM free magnesium). The standard reaction buffer was supplemented (for details see Supplementary Table 1) to assay the kinetics of the different enzymes. Data was processed using MatLab v.2011a. Absorbance values for controls were subtracted from absorbance of corresponding reactions. Gradients ($\text{absorbance}/\text{time}$) of the linear portion of the initial rates were calculated and divided by the extinction coefficient of NADH/NADPH (6.220 $\text{mM}^{-1}\text{cm}^{-1}$) to give the initial rate V_o values. Absorbance readings were normalised to give a path length of 1cm. Initial (V_o) rates were calculated using KINETICSWIZARD [40]. Graphpad prism 6 was used to plot V_o values against substrate concentration and determine V_{max} and K_m values. The V_{max} was then normalised to the protein concentration in the cell lysate.

Tumour responses *in vivo*

Adult (8 weeks +) female CD-1 nude mice (Charles River, Wilmington, MA, USA) were implanted with 0.1ml of H526 cells at 5×10^7 cells ml^{-1} . Cells were implanted subcutaneously in the mid-dorsal region and when tumour volumes reached 150mm^3 the mice were assigned treatment groups (up to 8 mice per group) and tumour measurements subsequently made daily. 100mg/kg AZD3965 was administered bi-daily by oral gavage for a total of seven days. This drug dose was chosen on the basis of being well tolerated and maintaining MCT1 inhibition over a seven day period [39]. On the third day of drug or vehicle treatment mice received 2Gy locally to the tumour for three successive days ($3 \times 2\text{Gy}$). In the radiation alone group the radiation was administered on the third day after the tumour volume reached 150mm^3 . Radiation treatment was given using a metal-ceramic MXR-320/36 X-ray machine (320kV, Comet AG, Switzerland) as previously described [42]. At the end of the seven day treatment period, three mice from each group were sacrificed for histological analysis of tumours. The remaining mice in each group were kept on study until tumours reached a volume of 1000mm^3 .

Animal study protocols were approved by the Institutional Ethics Committee and the Home Office (project license 40/3212,) and designed in accordance with the Scientific Procedures Act (1986) and the 2010 guidelines for the welfare and use of animals in cancer research [43].

IHC analysis

Tumours were harvested and snap frozen in two pieces in liquid nitrogen within 2 minutes of sacrifice. The tumours were cut into $10\mu\text{m}$ sections using a OFT5000 cryostat (Bright, Huntingdon, UK), fixed in chilled acetone and stained for MCT1, MCT4 (in-house [AstraZeneca] polyclonal antibodies), and CD31 (rat anti-mouse CD31, Pharmingen, BD Biosciences).

Statistics

Kaplan-Meier plots were evaluated using the log-rank (Mantel-Cox) test; otherwise significance was determined using an unpaired two tailed student's T-test for two-sample equal variance.

Results

AZD3965 inhibits bidirectional lactate transport

AZD3965 (supplementary Figure 1) was designed to selectively inhibit MCT1 and would therefore be expected to influence the movement of lactate into and out of cells. In the first instance, the effect of AZD3965 on lactate efflux was studied. Equivalent numbers of cells were incubated in either normoxia, 1% oxygen (hypoxia) or anoxia in complete media supplemented with AZD3965 or DMSO vehicle for 24 hours. After this time media and cells were collected to determine lactate concentrations. Generally, treatment with AZD3965 caused an increase in intracellular lactate (Figure 1A-C). There was a corresponding trend for reduction of extracellular lactate concentration, but these changes were not significantly

different; this may have been due to the inherent difficulty in measuring extracellular lactate in media which already contains significant amounts of serum-derived lactate (Figure 1D-F).

As MCT1 is a bidirectional transporter [13] the effects of AZD3965 on lactate influx were determined using a radioactive assay that measured the amount of lactate taken up by the cell (when other respiratory substrates were available) over one hour. Figure 2 (panels A and B) shows the effect of 24 hour treatment with AZD3965 on subsequent uptake of lactate. A significant decrease in lactate uptake was observed when the drug was administered 24 or 4 hours prior to, or the same time as, the radioactive lactate (defined as acute in Figure 2E and F). These experiments suggest that AZD3965 inhibits lactate transport by MCT1 regardless of the direction of lactate movement. Figure 2 also shows that inhibition of lactate uptake was seen when the hypoxia mimetic cobalt chloride was applied to the cells concurrently with AZD3965, this suggests that the HIF-1 mediated induction of MCT4 does not counteract the effect of the drug on lactate influx. This also suggests that even in the hypoxic regions of tumours, where MCT4 might be up-regulated, there might be significant inhibition of lactate uptake.

It is possible that the reduction in lactate uptake could contribute to the reduction in lactate efflux. This is because the reduction in lactate uptake creates a requirement for increased glycolysis to supply TCA cycle substrates, which must be immediately used by, and not lost from, the cell.

Metabolic analysis of the effect of inhibiting lactate transport

In order to determine the effects of inhibiting lactate transport on other metabolic pathways, 116 intracellular metabolites were analysed using LC-MS (for details see supplementary information). Samples were prepared 6 and 24 hours after the addition of 10nM or 1µM AZD3965 or DMSO control in both normoxia and hypoxia. A hierarchical analysis of the levels of individual metabolites under each experimental condition is provided in Supplementary Figure 2. The data were processed using an in-house model (the AstraZeneca pathway annotation tool). This model considered 41 metabolic pathways and the change in metabolite levels in each pathway was calculated. In this analysis, the extent to which a pathway is altered is determined by measuring the number of metabolites that demonstrate a significant change (see below) between the two samples that are being compared (indicated on the left hand side of the heat map in Figure 3). The greater the alteration, the brighter the colour assigned on the heat map. Larger changes in metabolism were observed when the treatment with AZD3965 was conducted under hypoxic conditions consistent with the increased requirement for lactate transport under these conditions. Also, greater changes were observed when the drug treatment was relatively short (6hr) as opposed to longer exposure times (24hr).

In the hypoxic samples, significant changes were observed in pathways involved in amino acid metabolism, such as: alanine, aspartate, glutamine, arginine, proline and β -alanine, as well as amino-acyl tRNA biosynthesis and amino acid and nucleotide sugar metabolism. These data are consistent with previous reports of a shift to an anabolic phenotype caused by oxidative stress mediated by effects on the pentose phosphate pathway (PPP) [44, 45]. Consistent with this, changes in PPP were also observed.

In order to consider whether the increased effects seen in the hypoxic samples are simply a reflection of the metabolic changes brought about by the hypoxic environment, the hypoxic samples were compared with their normoxic counterparts (matched for time and drug concentration). This analysis (shown in Supplementary Figure 3) also demonstrated evidence of a shift to an anabolic phenotype. This suggests that the comparable shift brought about by the drug could be as a result a heightened sensitivity of the cells to hypoxia as a result of treatment with AZD3965. Hypoxia also resulted in some changes to glycolytic intermediates, however, changes in glycolysis as a result of treatment with AZD3965 were observed in every 6hr time-point. Inspection of the individual metabolite levels indicated that there was a dose dependant increase in the concentration of intermediates early in the glycolytic pathway, and a similar dose dependant decrease in those appearing late (for example, pyruvate seen in Figure 4). The metabolite changes observed as a result of the treatment with AZD3965 are in the same direction as, but lesser in magnitude compared to the changes caused by hypoxia. As hypoxia is generally associated with an increase in glycolytic rate, this would suggest that the changes seen are indicative of a more glycolytic phenotype [46]. The drug-dose dependant nature of these changes, coupled with fact that there are dose dependant increases in both of the early glycolytic intermediates measured (glucose-6-phosphate and fructose-1-phosphate, see Figure 4), provide confidence in this conclusion.

We then analysed the effect of inhibiting lactate transport on glycolytic enzyme kinetics (Figure 4). Changes in V_{max} of both pyruvate kinase and hexokinase were demonstrated, however, for hexokinase there was no accompanying change in K_m , and the K_m change with pyruvate kinase was lower than the change in V_{max} . Increases in V_{max} indicate changes not in the kinetics of the enzyme reaction, but in the amount of enzyme present. These changes are particularly noticeable in the case of Hexokinase, the first enzyme in the glycolytic cascade. An up-regulation of hexokinase protein expression would be consistent with the increases in concentration of glucose-6-phosphate and fructose-1-phosphate. These expression changes would suggest that there has been a fundamental metabolic shift resulting in increased glycolysis in response to inhibition of lactate transport by AZD3965.

AZD3965 treatment results in increased oxidative stress

The metabolic changes observed above suggested that treatment of cells with AZD3965 could result in changes in cellular redox and cause oxidative stress. To evaluate this, we measured cellular levels of ATP, GSH/GSSG and the generation of reactive oxygen species (ROS) following treatment of cells with AZD3965 in air, hypoxia and anoxia (results are given in supplementary Figure 4). Anoxia alone results in a 50% reduction in cellular ATP and AZD3965 appears to cause a further decrease in ATP; in normoxia, 1 μ M AZD3965 causes a statistically significant 30% reduction in ATP. We further evaluated levels of GSH and GSSG; in air, AZD3965 has little effect on glutathione levels whereas in hypoxia a drug-dependent increase in the level of GSSG is observed. These changes in cellular redox were broadly reflected by the generation of ROS. In air, there was a decrease in ROS production following treatment with 1 μ M AZD3965, whereas in anoxia drug treatment led to a 50% increase in ROS. The different effects in air and anoxia probably indicate the different requirement of lactate transport under the different conditions. Interestingly, these

changes in redox and ROS production are not sufficient to mediate cytotoxicity (Supplementary methods and Supplementary Figure 5).

Treatment of tumours *in vivo* with AZD3965 causes increased lactate concentration, a reduction in growth and increased radiation sensitivity

Using conventional *in vitro* culture conditions, where glucose is abundant, cells are better able to compensate for the inhibition of lactate uptake. In contrast in tumours, cells are exposed to nutrient (oxygen) limitations as cells move further way from a functional vascular supply. Under these conditions it is likely that the use of lactate as a respiratory substrate is critical for tumour cell survival. This concept of metabolic symbiosis has been described by Sonveaux *et al.* [24], who suggested that hypoxic cells undergoing glycolysis will provide the aerobic fraction of a tumour with lactate to use as a respiratory substrate. This symbiosis has two advantages, firstly this allows the hypoxic, glycolytic fraction to benefit from sufficient glucose, but it also prevents acidification of the extracellular space that could be caused by lactate accumulation. In this model, MCT1 is likely to be pivotal to this shuttling of lactate between tumour compartments; hence the efficacy of AZD3965 was investigated *in vivo*.

Mice bearing H526 tumours were treated with AZD3965 for seven days. Figure 5A shows that treatment with AZD3965 resulted in a delay in tumour growth. Analysis of the time taken for individual tumours to grow from 150mm³ to 1000mm³ showed that this was 8 days for tumours in mice treated with vehicle alone compared to 12 days for those given AZD3965 (P = 0.004, Figure 5B). One mouse in the treatment group was cured and omitted from this analysis. However, a Kaplan-Meier plot of AZD3965 treatment efficacy, where survival was linked to tumour size (with animals sacrificed when tumours reached 1000mm³), also showed significance (P = 0.008). Tumours were harvested at the end of drug treatment, and at this time, higher concentrations of tumour lactate were found in the group that had received the AZD3965 suggesting *in vivo* efficacy in inhibiting lactate transport (Figure 6A). In order to ensure that this difference was not due to changes in angiogenesis, IHC analysis of CD31 was used to assess vessel number, size and overall coverage. Figure 6B shows there were no significant drug-induced changes in vessel number and similarly there were no changes in vessel size or coverage (Supplementary Figure 6). Thus, it is likely that the changes in lactate observed were a specific effect of MCT inhibition and not due to any changes in angiogenesis. Interestingly, a significant (p<0.05) increase was observed in the extent of MCT4 staining (Figure 6C) and this occurred without an increase hypoxia, as measured by Pimonidazole binding (data not shown), suggesting that the up regulation of MCT4 is not due to increased tumour hypoxia but rather indicative of increased glycolysis. This is consistent with our *in vitro* observations and the use of MCT4 as a glycolytic marker which has been published previously [47].

We have shown above that treatment of anoxic cells with AZD3965 can profoundly alter their redox status. This, together the fact that AZD3965 will perturb the metabolic symbiosis between the hypoxic and aerobic cells within the tumour, strongly suggests that the hypoxic/anoxic cells may be more vulnerable to adjuvant treatment. Since the effectiveness of radiotherapy is limited by the resistance of the hypoxic/anoxic cells [1], a combination of

AZD3965 with radiotherapy could be beneficial. To test this, H526 xenografts were grown to a volume of 150mm³; one group of mice received no treatment for two days followed by three daily fractions of 2Gy (3×2Gy); the second group received AZD3965 for two days followed by AZD3965 together with 3×2Gy fractionated radiotherapy followed by two further days of AZD3965. Mice were sacrificed at the end of drug treatment or tumours were allowed to grow to 1000mm³. In all cases, tumours were harvested for IHC analysis or assessment of lactate levels. At the end of the treatment period there was a considerable increase in the lactate levels observed in the tumours treated with AZD3965 (Figure 7A). By comparison with Figure 6, radiation alone has no discernible effect on tumour lactate levels.

Administration of AZD3965 alone for seven days increased the time for tumours to reach 1000mm³ from 8 to 12 days (Figure 5); for radiation alone this time was 18 days, which was increased to 25 days when combined with AZD3965 (P = 0.02, Figure 7B). Growth curves are given in (Figure 7C). Kaplan-Meier analysis (Figure 7D) showed that the difference in survival between the mice treated with radiation only compared to the group receiving radiation plus AZD3965 was significant (P = 0.011). Clearly, the therapeutic effect of combining AZD3965 with radiotherapy is greater than using either modality individually.

Discussion

Sonveaux *et al.* [24] used the non-specific MCT1 inhibitor CHC to propose a model whereby inhibition of lactate influx resulted in a switch from lactate fuelled oxidative metabolism to glycolysis in the oxygenated regions of the tumour. They demonstrated that, in oxygenated regions, lactate was used as a fuel source in preference to glucose while, when MCT1 was inhibited, the cells adopted a glycolytic phenotype using glucose as their fuel source. These data were of considerable importance for highlighting the potential therapeutic importance of inhibiting lactate transport; however, despite the rigorous controls employed by the authors there were still some concerns about the overall conclusions as CHC is not a specific inhibitor of MCT1. One of the off-target effects of CHC is inhibition of the mitochondrial pyruvate carrier. This inhibition is possible at the concentrations used in the study by Sonveaux *et al.* [24], and could explain the inhibition of lactate oxidation observed [34]. In contrast, AZD3965 is a specific MCT1 inhibitor and therefore, we are able to demonstrate, unambiguously, that the abrogation of the symbiotic tumour microenvironment can be achieved by the inhibition of lactate transport by MCT1.

We have demonstrated that AZD3965 is able to inhibit lactate transport both into and out of the cell with the greater effect observed on lactate uptake. These data are concordant with the majority of published observations regarding the role of MCT1 in lactate transport [13, 15, 24, 48] and thus treatment with AZD3965 will restrict lactate availability as a fuel source for aerobic metabolism. This metabolic change would force those cells utilizing lactate to use an alternative fuel e.g. glucose, thus increasing the rate of glycolysis. This hypothesis is supported by the observation that treatment with AZD3965 resulted in changes in glycolytic metabolites determined by metabolomics analysis, an up regulation of glycolytic enzymes measured by glycolytic flux analysis, and an increase in the rate of glucose uptake (although this was not statistically significant). In keeping with this, the increase in cellular lactate that is observed could be due to an increase in glycolysis.

Inhibition of lactate transport resulted in a significant increase in tumour lactate *in vivo* and this effect was not as a result of perfusion changes brought about by changes to the blood vessels in the tumour. Moreover at the end of the treatment period a significant increase in MCT4 staining was observed; MCT4 is often considered a marker of glycolysis [47], and as such is concordant with previous observations surrounding increases in glycolytic rate. Despite the relatively brief treatment period (seven days), AZD3965 was also able to produce a statistically significant inhibition of tumour growth as a monotherapy.

On the basis of our hypotheses, AZD3965 would be particularly effective at killing the hypoxic areas of the tumour, as these would be the areas that would be starved of glucose when the aerobic fraction is unable to use lactate as a metabolic substrate. Moreover, the reduced cellular ATP, the increased percentage of GSSG and the increase in ROS in anoxic conditions are indicative of cells experiencing oxidative stress and as such these cells would be more sensitive to radiotherapy. As a consequence, AZD3965 was combined with radiotherapy. When mice bearing tumours were treated with AZD3965 concurrently with 3×2Gy radiotherapy and with AZD3965 alone for two days either side of the radiation treatment, a significant decrease in tumour growth was observed in the AZD3965 combined with radiation group when compared to the groups that received either drug or radiation alone.

There is recent work describing the potential importance of metabolic symbiosis as important factor for sustaining tumour growth [49]. It is likely that treatment of tumours with AZD3965 will perturb this symbiosis with the result of decreased tumour growth and enhancement of the effects of radiotherapy. Inhibition of MCT1 with AZD3965 represents a novel method of specifically targeting solid tumours by pinpointing weaknesses inherent in the tumour microenvironment and this suggests that systemic administration in combination with targeted radiotherapy could represent an effective therapeutic strategy.

Supplementary Material

Refer to Web version on PubMed Central for supplementary material.

Acknowledgements

We thank Mike Firth for the use of the metabolic network viewer, Radoslaw Polanski and Christopher Morrow for their helpful discussions and the Faculty of Life Sciences, the University of Manchester for making available the FACS and microscopy core facilities. The work was funded by grants (to IJS) from the MRC (G0500366) and AstraZeneca. The award of PhD studentships by BBSRC to ALC and KGB is gratefully acknowledged.

Funding for this research: A Research grant from AstraZeneca (to I.J. Stratford) provided the support for this work. Additional funding came from the MRC (G0500366).

References

1. Gray LH, Conger AD, Ebert M, Hornsey S, Scott OCA. The concentration of oxygen dissolved in tissues at the time of irradiation as a factor in radiotherapy. *Br J Radiol.* 1953; 26(312):638–48. [PubMed: 13106296]
2. Karar J, Maity A. Modulating the tumor microenvironment to increase radiation responsiveness. *Cancer Biol Ther.* 2009; 8(21):1994–2001. [PubMed: 19823031]

3. Koch CJ, Kruuv J, Frey HE. Variation in radiation response of mammalian cells as a function of oxygen tension. *Radiat Res.* 1973; 53(1):33–42. [PubMed: 4734388]
4. Yasuda H. Solid tumor physiology and hypoxia-induced chemo/radio-resistance: novel strategy for cancer therapy: nitric oxide donor as a therapeutic enhancer. *Nitric Oxide.* 2008; 19(2):205–16. [PubMed: 18503779]
5. Pavlides S, Whitaker-Menezes D, Castello-Cros R, Flomenberg N, Witkiewicz AK, Frank PG, et al. The reverse Warburg effect: aerobic glycolysis in cancer associated fibroblasts and the tumor stroma. *Cell Cycle.* 2009; 8(23):3984–4001. [PubMed: 19923890]
6. Hanahan D, Weinberg RA. Hallmarks of cancer: the next generation. *Cell.* 2011; 144(5):646–74. [PubMed: 21376230]
7. Hirschhaeuser F, Sattler UG, Mueller-Klieser W. Lactate: a metabolic key player in cancer. *Cancer Res.* 2011; 71(22):6921–5. [PubMed: 22084445]
8. Fulham MJ, Bizzi A, Dietz MJ, Shih HH, Raman R, Sobering GS, et al. Mapping of brain tumor metabolites with proton MR spectroscopic imaging: clinical relevance. *Radiology.* 1992; 185(3):675–86. [PubMed: 1438744]
9. Hossmann KA, Mies G, Paschen W, Szabo L, Dolan E, Wechsler W. Regional metabolism of experimental brain tumors. *Acta Neuropathol.* 1986; 69(1-2):139–47. [PubMed: 3962590]
10. Kennedy KM, Dewhirst MW. Tumor metabolism of lactate: the influence and therapeutic potential for MCT and CD147 regulation. *Future Oncol.* 2010; 6(1):127–48. [PubMed: 20021214]
11. Paschen W, Djuricic B, Mies G, Schmidt-Kastner R, Linn F. Lactate and pH in the brain: association and dissociation in different pathophysiological states. *J Neurochem.* 1987; 48(1):154–9. [PubMed: 3794696]
12. Yokota H, Guo J, Matoba M, Higashi K, Tonami H, Nagao Y. Lactate, choline, and creatine levels measured by *in vitro* 1H-MRS as prognostic parameters in patients with non-small-cell lung cancer. *J Magn Reson Imaging.* 2007; 25(5):992–9. [PubMed: 17410583]
13. Halestrap AP, Price NT. The proton-linked monocarboxylate transporter (MCT) family: structure, function and regulation. *Biochem J.* 1999; 343(Pt 2):281–99. [PubMed: 10510291]
14. Ovens MJ, Davies AJ, Wilson MC, Murray CM, Halestrap AP. AR-C155858 is a potent inhibitor of monocarboxylate transporters MCT1 and MCT2 that binds to an intracellular site involving transmembrane helices 7-10. *Biochem J.* 2010; 425(3):523–30. [PubMed: 19929853]
15. Halestrap AP, Meredith D. The SLC16 gene family—from monocarboxylate transporters (MCTs) to aromatic amino acid transporters and beyond. *Pflugers Arch.* 2004; 447(5):619–28. [PubMed: 12739169]
16. Juel C, Halestrap AP. Lactate transport in skeletal muscle - role and regulation of the monocarboxylate transporter. *J Physiol.* 1999; 517(Pt 3):633–42. [PubMed: 10358105]
17. Ullah MS, Davies AJ, Halestrap AP. The plasma membrane lactate transporter MCT4, but not MCT1, is up-regulated by hypoxia through a HIF-1alpha-dependent mechanism. *J Biol Chem.* 2006; 281(14):9030–7. [PubMed: 16452478]
18. Bonen A. The expression of lactate transporters (MCT1 and MCT4) in heart and muscle. *Eur J Appl Physiol.* 2001; 86(1):6–11. [PubMed: 11820324]
19. Dubouchaud H, Butterfield GE, Wolfel EE, Bergman BC, Brooks GA. Endurance training, expression, and physiology of LDH, MCT1, and MCT4 in human skeletal muscle. *Am J Physiol Endocrinol Metab.* 2000; 278(4):E571–9. [PubMed: 10751188]
20. Manning Fox JE, Meredith D, Halestrap AP. Characterisation of human monocarboxylate transporter 4 substantiates its role in lactic acid efflux from skeletal muscle. *J Physiol.* 2000; 529(Pt 2):285–93. [PubMed: 11101640]
21. Bergersen LH. Is lactate food for neurons? Comparison of monocarboxylate transporter subtypes in brain and muscle. *Neuroscience.* 2007; 145(1):11–9. [PubMed: 17218064]
22. Brooks GA. Lactate shuttles in nature. *Biochem Soc Trans.* 2002; 30(2):258–64. [PubMed: 12023861]
23. Pellerin L. Lactate as a pivotal element in neuron-glia metabolic cooperation. *Neurochem Int.* 2003; 43(4-5):331–8. [PubMed: 12742077]

24. Sonveau, x P.; Végran, F.; Schroeder, T.; Wergin, MC.; Verrax, J.; Rabbani, ZN., et al. Targeting lactate-fueled respiration selectively kills hypoxic tumor cells in mice. *J Clin Invest.* 2008; 118(12):3930–42. [PubMed: 19033663]
25. Martinez-Outschoorn UE, Balliet RM, Lin Z, Whitaker-Menezes D, Howell A, Sotgia F, et al. Hereditary ovarian cancer and two-compartment tumor metabolism: epithelial loss of BRCA1 induces hydrogen peroxide production, driving oxidative stress and NFkappaB activation in the tumor stroma. *Cell Cycle.* 2012; 11(22):4152–66. [PubMed: 23047606]
26. Fiaschi T, Chiarugi P. Oxidative stress, tumor microenvironment, and metabolic reprogramming: a diabolic liaison. *Int J Cell Biol.* 2012; 2012 ID. 762825.
27. Pinheiro C, Albergaria A, Paredes J, Sousa B, Dufloth R, Vieira D, et al. Monocarboxylate transporter 1 is up-regulated in basal-like breast carcinoma. *Histopathology.* 2010; 56(7):860–7. [PubMed: 20636790]
28. Chen H, Wang L, Beretov J, Hao J, Xiao W, Li Y. Co-expression of CD147/EMMPRIN with monocarboxylate transporters and multiple drug resistance proteins is associated with epithelial ovarian cancer progression. *Clin Exp Metastasis.* 2010; 27(8):557–69. [PubMed: 20658178]
29. Pinheiro C, Longatto-Filho A, Simões K, Jacob CE, Bresciani CJ, Zilberstein B, et al. The prognostic value of CD147/EMMPRIN is associated with monocarboxylate transporter 1 co-expression in gastric cancer. *Eur J Cancer.* 2009; 45(13):2418–24. [PubMed: 19628385]
30. Pinheiro C, Longatto-Filho A, Scapulatempo C, Ferreira L, Martins S, Pellerin L, et al. Increased expression of monocarboxylate transporters 1, 2, and 4 in colorectal carcinomas. *Virchows Arch.* 2008; 452(2):139–46. [PubMed: 18188595]
31. Kim HS, Masko EM, Poulton SL, Kennedy KM, Pizzo SV, Dewhirst MW, et al. Carbohydrate restriction and lactate transporter inhibition in a mouse xenograft model of human prostate cancer. *BJU Int.* 2012; 110(7):1062–9. [PubMed: 22394625]
32. Miranda-Gonçalves V, Honavar M, Pinheiro C, Martinho O, Pires MM, Pinheiro C, et al. Monocarboxylate transporters (MCTs) in gliomas: expression and exploitation as therapeutic targets. *Neuro Oncol.* 2013; 15(2):172–88. [PubMed: 23258846]
33. Colen CB, Shen Y, Ghoddoussi F, Yu P, Francis TB, Koch BJ, et al. Metabolic targeting of lactate efflux by malignant glioma inhibits invasiveness and induces necrosis: an in vivo study. *Neoplasia.* 2011; 13(7):620–32. [PubMed: 21750656]
34. Halestrap AP. e-letter: Inhibiting lactate oxidation in tumor cells. *J. of Clin. Invest.* 2008; 118(12): 3930–3942. [PubMed: 19033663]
35. Busk M, Walenta S, Mueller-Klieser W, Steiniche T, Jakobsen S, Horsman MR, et al. Inhibition of tumor lactate oxidation: consequences for the tumor microenvironment. *Radiother Oncol.* 2011; 99(3):404–11. [PubMed: 21704401]
36. Bueno V, Binet I, Steger U, Bundick R, Ferguson D, Murray C, et al. The specific monocarboxylate transporter (MCT1) inhibitor, AR-C117977, a novel immunosuppressant, prolongs allograft survival in the mouse. *Transplantation.* 2007; 84(9):1204–7. [PubMed: 17998878]
37. Ekberg H, Qi Z, Pahlman C, Veress B, Bundick RV, Craggs RI, et al. The specific monocarboxylate transporter-1 (MCT-1) inhibitor, AR-C117977, induces donor-specific suppression, reducing acute and chronic allograft rejection in the rat. *Transplantation.* 2007; 84(9): 1191–9. [PubMed: 17998876]
38. Le Floch R, Chiche J, Marchiq I, Naiken T, Ilic K, Murray CM, et al. CD147 subunit of lactate/H⁺ symporters MCT1 and hypoxia-inducible MCT4 is critical for energetics and growth of glycolytic tumors. *Proc Natl Acad Sci U S A.* 2011; 108(40):16663–8. [PubMed: 21930917]
39. Critchlow, SE.; Hopcroft, L.; Mooney, L.; Curtis, N.; Whalley, N.; Zhong, H., et al. Pre-clinical targeting of the metabolic phenotype of lymphoma by AZD3965, a selective inhibitor of monocarboxylate transporter 1 (MCT1); AACR Annual Meeting Proceedings; 2012; abstr 3224
40. <http://science.cancerresearchuk.org/>
41. Swainston N, Golebiewski M, Messiha HL, Malys N, Kania R, Kengne S, et al. Enzyme kinetics informatics: from instrument to browser. *Febs J.* 2010; 277(18):3769–79. [PubMed: 20738395]
42. Williams KJ, Telfer BA, Shannon AM, Babur M, Stratford IJ, Wedge SR. Combining radiotherapy with AZD2171, a potent inhibitor of vascular endothelial growth factor signaling:

- pathophysiologic effects and therapeutic benefit. *Mol Cancer Ther.* 2007; 6(2):599–606. [PubMed: 17308057]
43. Workman P, Aboagye EO, Balkwill F, Balmain A, Bruder G, Chaplin DJ, et al. Guidelines for the welfare and use of animals in cancer research. *Br J Cancer.* 2010; 102(11):1555–77. [PubMed: 20502460]
 44. Bensaad K, Tsuruta A, Selak MA, Vidal MN, Nakano K, Bartrons R, et al. TIGAR, a p53-inducible regulator of glycolysis and apoptosis. *Cell.* 2006; 126(1):107–20. [PubMed: 16839880]
 45. Gottlieb E, Vousden KH. p53 regulation of metabolic pathways. *Cold Spring Harb Perspect Biol.* 2010; 2(4):a001040. [PubMed: 20452943]
 46. Semenza GL. Regulation of metabolism by hypoxia-inducible factor 1. *Cold Spring Harb Symp Quant Biol.* 2011; 76:347–53. [PubMed: 21785006]
 47. Whitaker-Menezes D, Martinez-Outschoorn UE, Lin Z, Ertel A, Flomenberg N, Witkiewicz AK, et al. Evidence for a stromal-epithelial “lactate shuttle” in human tumors: MCT4 is a marker of oxidative stress in cancer-associated fibroblasts. *Cell Cycle.* 2011; 10(11):1772–83. [PubMed: 21558814]
 48. Halestrap AP. The monocarboxylate transporter family--Structure and functional characterization. *IUBMB Life.* 2012; 64(1):1–9. [PubMed: 22131303]
 49. Kennedy KM, Scarborough PM, Ribeiro A, Richardson R, Yuan H, Sonveaux P, et al. Catabolism of exogenous lactate reveals it as a legitimate metabolic substrate in breast cancer. *PLoS One.* 2013; 8(9):e75154. [PubMed: 24069390]

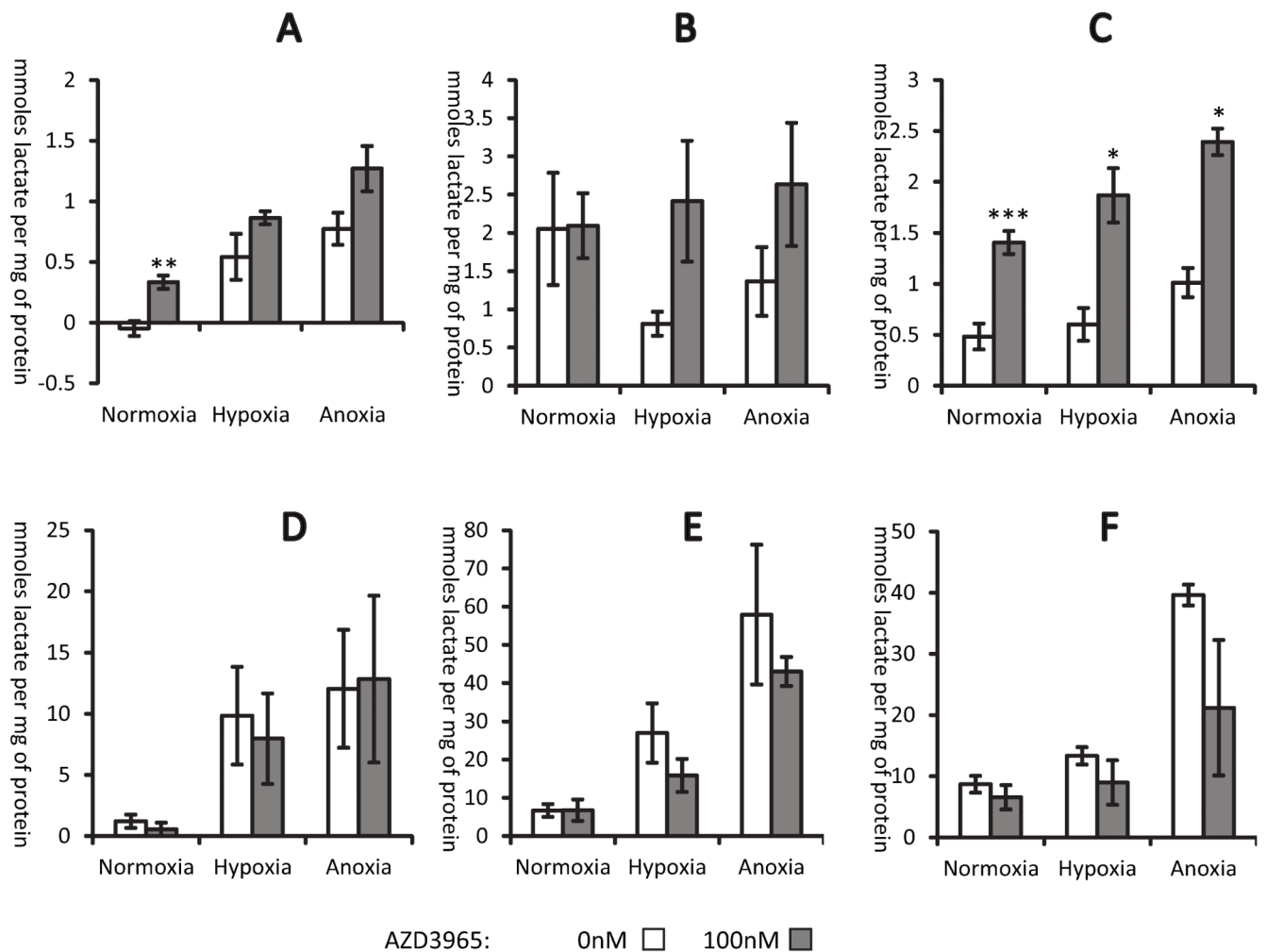


Figure 1. AZD3965 increases intracellular lactate whilst decreasing the amount of extracellular lactate

Cells were treated with 100nM AZD3965 in normoxia, hypoxia or anoxia for 24hrs prior to determining lactate concentrations. Intracellular lactate **A**), **B**) and **C**); extracellular lactate **D**), **E**) and **F**). H526 cells, **A**) and **D**); HGC27 cells, **B**) and **E**); DMS114 cells, **C**) and **F**). Significantly different; drug treated versus controls; *, **, ***, $P < 0.05$, $P < 0.01$, $P < 0.001$ respectively. Mean and SEMs are derived from 3 independent experiments.

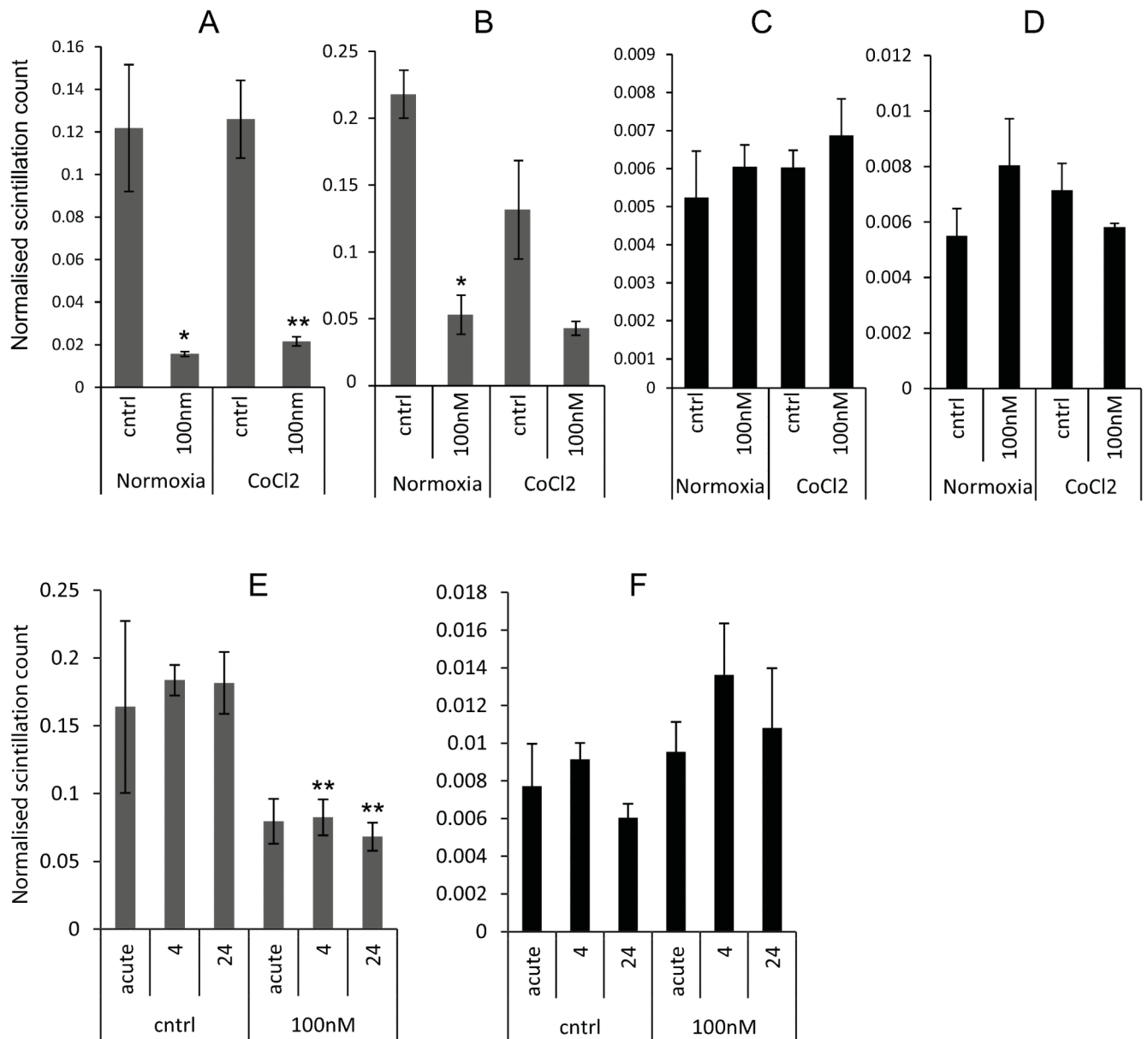


Figure 2. AZD3965 significantly reduces lactate uptake

The uptake of lactate (A and B) and glucose (C and D) was measured 24 hours after exposure to AZD3965 in the presence or absence of Cobalt Chloride. A and C DMS114 cells and B and D HGC27 cells. Panels E) and F) show time course assays, where AZD3965 was applied for the number of hours indicated; “acute” dosing is when drug was administered concomitant with radiolabelled metabolite. E) lactate, F) glucose. Significantly different; drug treated versus controls; *, **, P<0.05 and P<0.01, respectively. Mean and SEMs derived from 3 independent experiments.

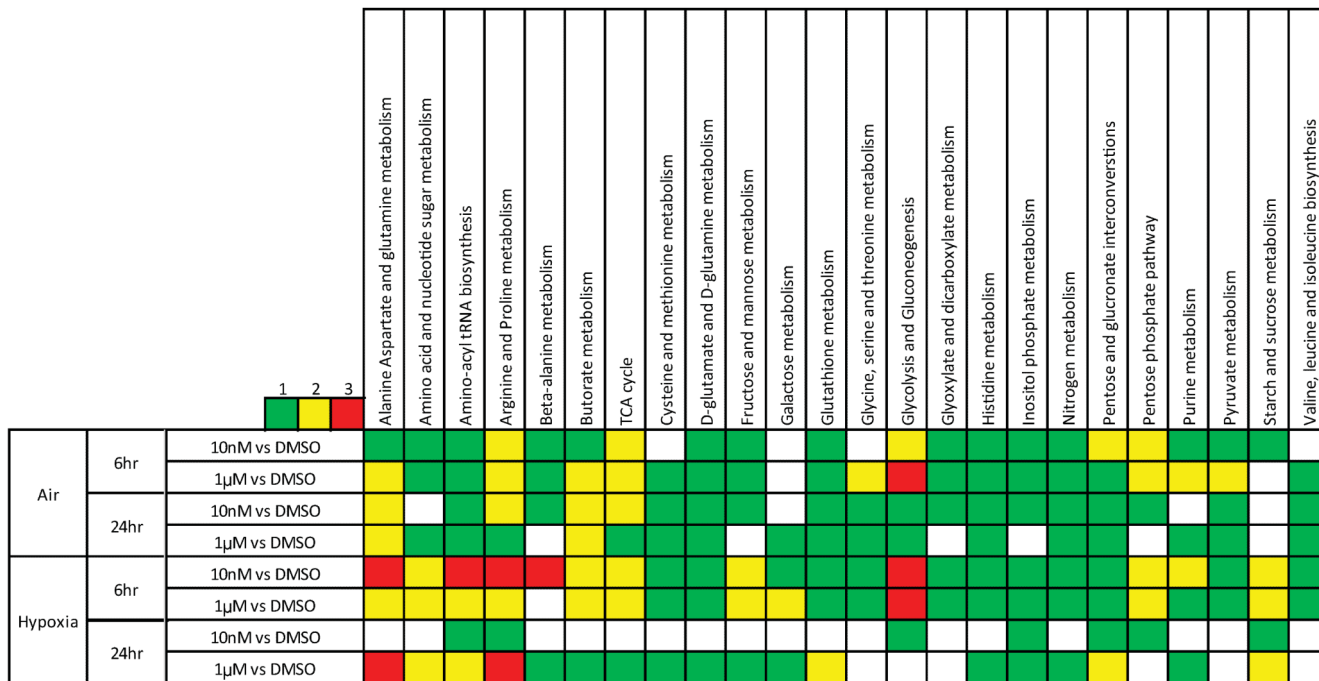


Figure 3. The effect of inhibiting lactate transport on metabolism
 The heat map represents the extent of change in a pathway when the two conditions indicated in the right hand column are compared. The colours indicate the number of the metabolites in that pathway that show a significant change in concentration. No weighting is given to the extent or the direction of the change in the levels of individual metabolites.

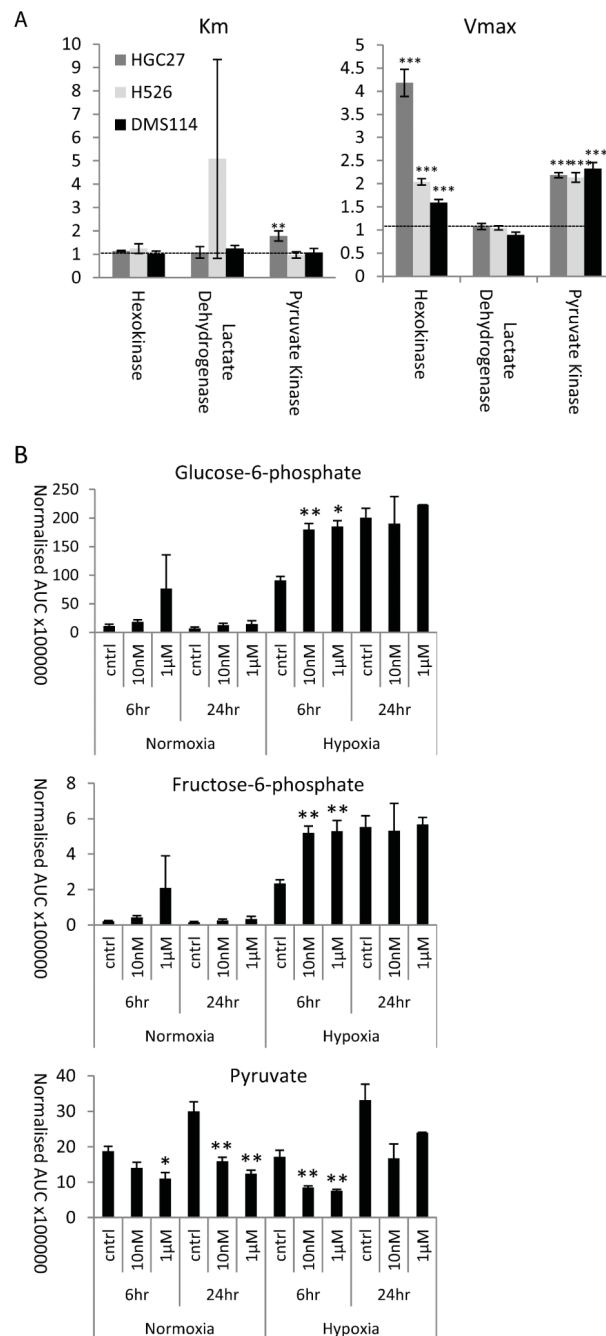


Figure 4. Inhibiting lactate transport increases glycolytic rate

A) Glycolytic flux analysis was used to compare the activity of three key glycolytic enzymes. Km and Vmax were calculated and are expressed as a ratio of the control cells to the cells treated for 24hr with 100nM AZD3965; the horizontal line indicates a value indicative of no change as a result of treatment with AZD3965. **B)** The concentrations of the individual metabolites measured in the glycolytic pathway (values represent area under curve (AUC) normalised to median AUC). Mean and SEMs derived from 3 independent

experiments. Significantly different; drug treated versus controls; *, **, ***, $P < 0.05$, $P < 0.01$ and $P < 0.001$ respectively.

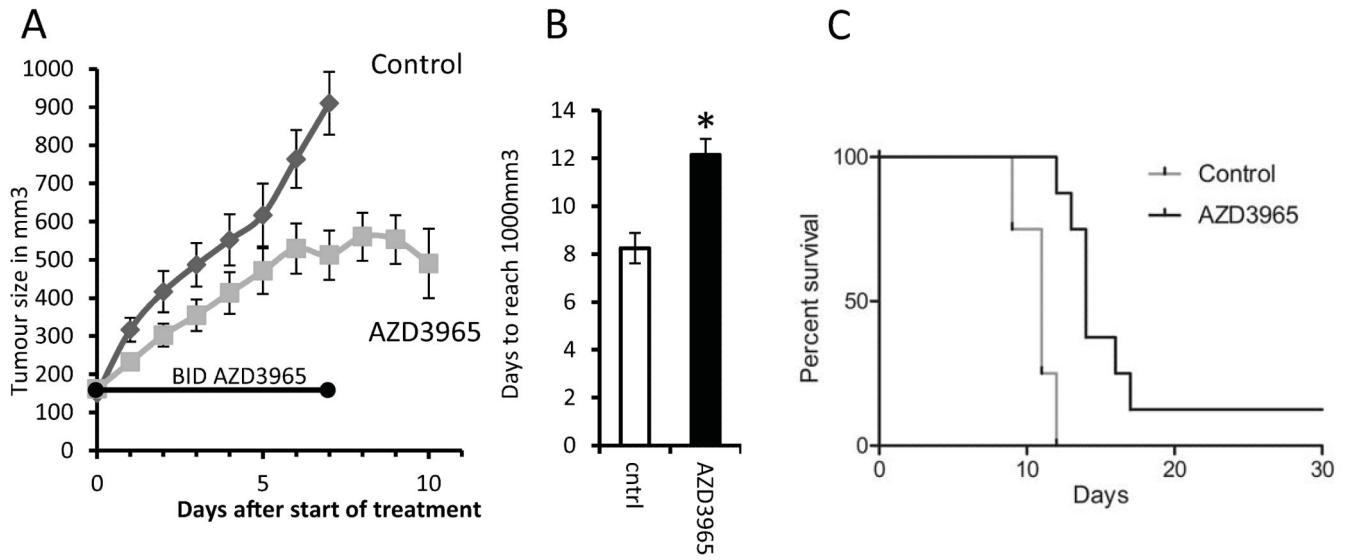


Figure 5. AZD3965 slows H526 xenograft growth *in vivo*

A) *In vivo* growth curves showing tumour volume (mean and SEM) in mm³ post start of treatment; the growth curve finishes when the first tumour in each group reaches 1000mm³. The control group contained 5 mice the AZD3965 group contained 11 mice three of which were sacrificed for histology at the end of drug treatment (day 7). **B)** Days (\pm SEM) taken to reach 1000mm³ for each treatment group (significantly different; *, P = 0.004). In the AZD3965 group one mouse was cured and observed for a further 100 days after the tumour ceased to be visible and no tumour returned. This reduction in tumour size resulted in the apparent dip at the end of the AZD3965 growth curve and is why the Kaplan-Meier plot (C) does not reach zero for the AZD3965 group.

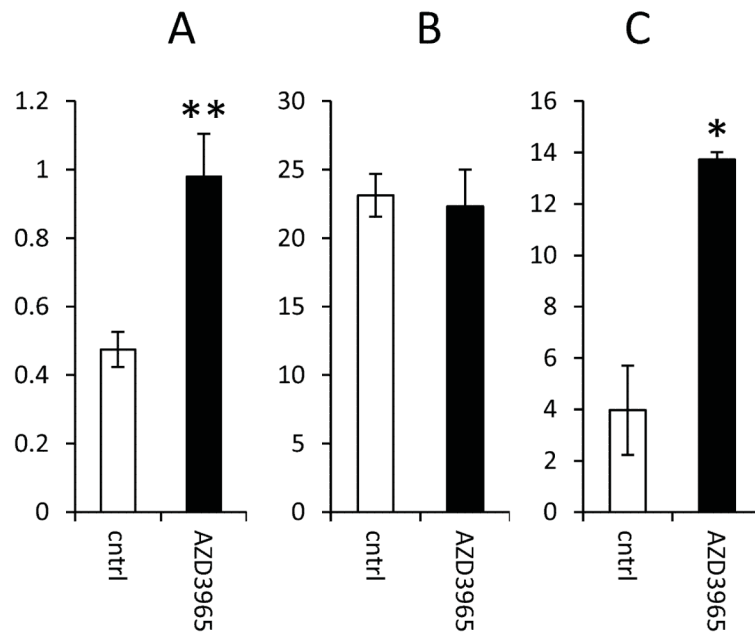


Figure 6. Effect of AZD3965 on lactate concentration, blood vessel density and MCT4 expression in H526 xenografts

A) Lactate concentration expressed as mM lactate per mg of protein; **B)** mean number of blood vessels per image of the tumour as visualised using the endothelial cell marker, CD31; **C)** proportion of tumour stained for MCT4. Significantly different; drug treated versus controls; *, **, $P < 0.05$ and $P < 0.01$ respectively.

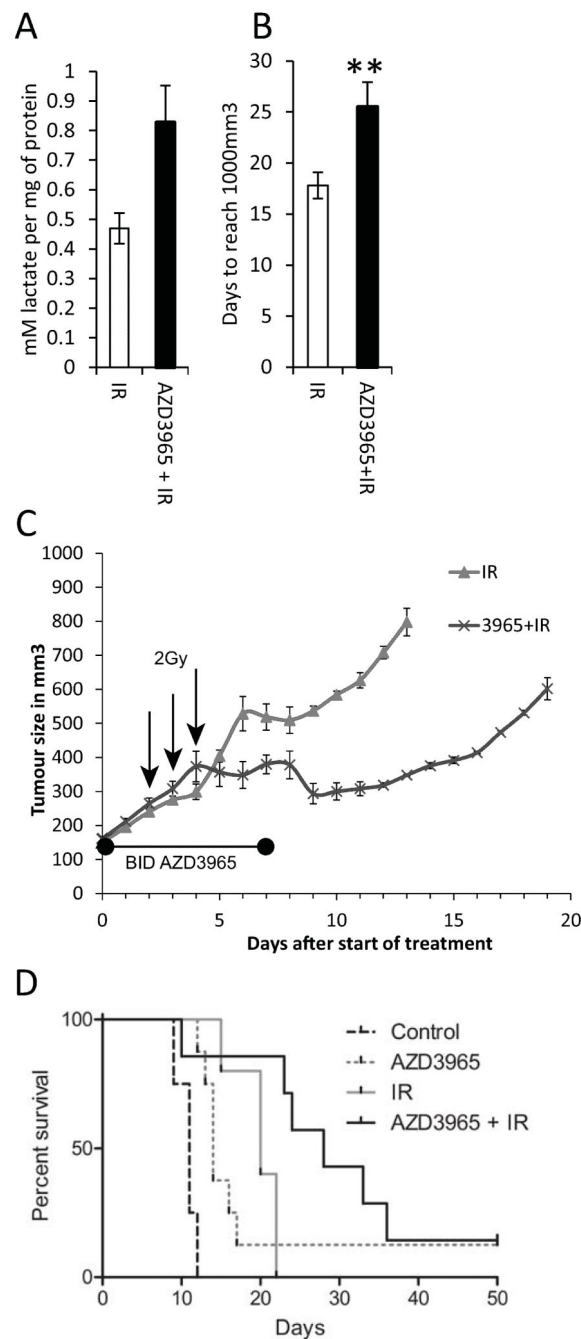


Figure 7. Combining AZD3965 with radiation to treat H526 xenografts

A) Tumour lactate concentration at the end of drug treatment ($P = 0.14$); **B)** Days taken to reach 1000mm^3 , (mean and SEM, cured tumour not included), significantly different; drug plus radiation versus radiation alone; **, $P = 0.02$. The radiation only group contained 8 mice 3 of which were sacrificed at the end of the treatment period (7 days) for histology, the radiation plus AZD3965 group contained 10 mice 3 of which were sacrificed at the end of drug treatment for histology. **C)** *In vivo* growth curves showing tumour volume in mm^3 (mean and SEM), the growth curve finishes when the first tumour reaches 1000mm^3 . The 2

Gy fractions of radiation were delivered midway between the two doses of AZD3965 on the days indicated with an arrow. In the AZD3965 + radiation group, one mouse was cured and observed for a further 100 days after the tumour ceased to be visible and no tumour returned. This is why the Kaplan-Meier plot (**D**) does not reach zero for the AZD3965 group; the dotted lines are taken from figure 5, with both experiments being carried out at the same time.